

The peculiarities of heat transfer in CO₂ and N₂O solids at low temperatures

V.V. Sumarokov

B. Verkin Institute for Low Temperature Physics and Engineering of the National Academy of Sciences of Ukraine
47 Lenin Ave., Kharkov 61103, Ukraine
E-mail: sumarokov@ilt.kharkov.ua

P. Stachowiak and A. Jeżowski

V. Trzebiatowski Institute of Low Temperature and Structure Research, Polish Academy of Sciences
P.O. Box 1410, 50-950 Wrocław, Poland
E-mail: p.stachowiak@int.pan.wroc.pl
a.jezowski@int.pan.wroc.pl

The thermal conductivities of CO₂ and N₂O solids have been investigated in the low-temperature range 1–40 K. The thermal conductivities of CO₂ and N₂O are large compared with those of simple molecular crystals such as N₂, CO, or O₂ in the whole investigated temperature range. Analysis of the experimental data by the Callaway method shows that relatively large size of crystalline grains, low density of dislocations and weak phonon–phonon interaction might be the reasons for the good thermal conduction in these crystals at temperatures near the maxima. A comparison between calculated values of the intensity of normal phonon scattering processes and experiment gives evidence that in N₂O there is an additional (in comparison with CO₂) giant scattering of phonons. This scattering is described in the frameworks of soft potential model by the resonance phonon scattering on tunnel states and low-energy vibratons.

PACS: **63.20.–e** Phonons in crystal lattices;
66.70.+f Nonelectronic thermal conduction and heat-pulse propagation in solids; thermal waves;
44.10.+i Heat conduction.

Keywords: thermal conductivity, heat transfer, molecular cryocrystals, dipolar disordered system.

Introduction

CO₂ and N₂O cryocrystals have much in common. They have close molecular and crystal parameters (molecular mass, spacing between nearest neighbors, zero-oscillation energies [1,2]).

Under equilibrium vapor pressure, CO₂ and N₂O have the *Pa3* crystal structure below their triple-point temperatures 216.57 and 182.35 K [1,2], respectively. The molecular axes in these crystals are oriented along the body diagonals of the cubic unit cell. The main distinction between solid CO₂ and N₂O is due to that the N₂O (N–N–O) molecule, unlike the CO₂ (O–C–O) one, is asymmetric. N₂O molecules are head-tail disoriented [3]. The residual entropy (difference between spectroscopic and calorimetric entropies) $\Delta S_{\text{res}}/R \ln 2 = 1.04 \pm 0.17$ (Ref. 4) indicates that this disorder persists at low temperatures.

The experimental investigation of the low-temperature thermal conductivity of CO₂ and N₂ crystals [5–7] reveals a very strong phonon scattering in the N₂O solid (in comparison with CO₂). By fitting a model to experimental curves, the authors of Ref. 7 found the expression for the relaxation time, allowing then to describe effectively the contribution of this extra (as compared to CO₂) phonon scattering to the thermal conductivity, as a function of the temperature and phonon frequency: $\tau_a^{-1} \sim \omega^{-1/5} T^2$. It was assumed that the additional thermal resistance was caused by phonon scattering on the head-tail disorder of N₂O molecules. The orientation of the N₂O axes along the cube body diagonal is practically frozen since the times of the 180° reorientation of the molecules are very long at low temperatures. These N₂O molecules, localized at their sites, can have one of two stable orientations that differ by 180° and are separated by a barrier. They form some-

thing like a two-level orientational subsystem. It is similar to an orientational glass, which influences the temperature behavior of the thermal conductivity. The typical properties of glasses usually manifest themselves below 1 K. The low-temperature properties are commonly described within a two-level system model [8]. In the low-temperature region ($T < 1$ K), the heat capacity is proportional to temperature, and the thermal conductivity is proportional to the temperature squared. The major contribution to the thermal conductivity of glasses in this temperature region comes from resonance scattering of phonons at two-level systems. In a wider temperature interval the properties of glasses can be described efficiently by the model of soft atomic potentials (SPM) [e.g., see Ref. 9 and references therein]. The role of the N-processes on heat transfer was not cleared in Ref. 7.

This study concerns the role of normal processes in heat transfer of CO₂ and N₂O cryocrystals.

Experiment

The thermal conductivity of CO₂ and N₂O crystals was measured using the steady-state flow method.

Since we meant to compare the thermal conductivities of these crystals, special attention was concentrated on the quality of the samples. A special technique was developed, which allowed us to prepare perfect crystalline samples of CO₂ and N₂O. The samples were grown and investigated in a cylindrical glass ampoule 36 mm high with an inner diameter of 4.2 mm.

The crystals were grown directly from the gas phase. The condensation temperature was about 173 and 162 K for CO₂ and N₂O, respectively. The growth rate was about 1.5 mm/h. The quality of the crystals is sensitive to the annealing and cooling conditions. Special effort was therefore made to exclude their effect upon the thermal conductivity in these crystals. Thus, the CO₂ sample and the last N₂O sample were cooled at a rate of ~ 0.1 K/h down to 100 K, ~ 0.2 K/h in the temperature range 100–70 K, and about 0.5 K/h below 70 K.

The sample growth could be monitored through special windows in the cryostat with the cold shields open. The crystalline CO₂ and N₂O samples were transparent, without visible defects after cooling to helium temperatures. The gases employed for sample growth had the natural isotopic composition. The impurity content was not higher than 0.001%.

The sample temperature and the temperature gradient over the sample were measured with germanium resistance thermometers placed at a 12 mm distance between them.

Other details of experiment are described elsewhere [5–7,10].

Results and discussion

The thermal conductivity of the N₂O and CO₂ crystals was measured in the interval 1–40 K. The experimental results [5–7] are shown in Fig. 1. It is interesting that (i) the maxima differ considerably in shape, (ii) the thermal conductivity coefficients of both crystals are very high at the maxima exceeding greatly the corresponding coefficients of simple molecular cryocrystals N₂ (Ref. 11), CO (Ref. 12) and O₂ (Ref. 13) whose thermal conductivity at the maximum is about 200 mW/(cm·K). The high value of the thermal conductivity at the maximum is due to the high degree of perfection of the N₂O and CO₂ samples and to the sound-velocity relationship in these crystals. The maximum in CO₂ is a sharply pointed peak. In the case of N₂O the maximum is broad as if it was cut off by additional phonon scattering. It was assumed [7] that the additional thermal resistance is caused by the phonon scattering at N₂O molecules, which are head-tail disordered. Phenomenologically, the relaxation time of the extra (as compared to the CO₂ crystal) scattering was estimated [7]. The authors did not allow for the contribution of normal processes to the thermal conductivity of these crystals.

Let us consider the effect of N-processes on the heat transfer in N₂O and CO₂ crystals and the heat transfer features related to the orientational N₂O subsystem. It is well known that N-processes play a special role in thermal conduction. Although they do not contribute to the ther-

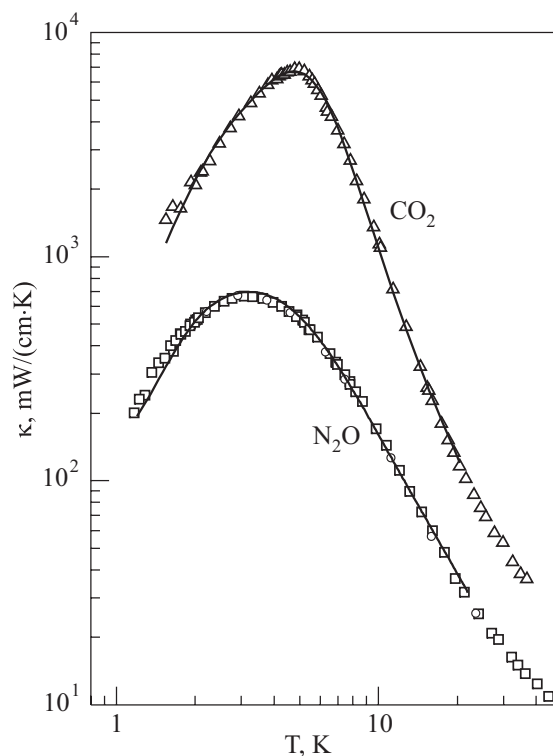


Fig. 1. The temperature dependence of the low-temperature thermal conductivities κ of CO₂ and N₂O solids. Experiment: N₂O (\square , \circ), CO₂ (\triangle). Solid curves: the best fitting.

mal resistance [14] directly, they participate in the energy redistribution in the phonon subsystem and thus affect thermal conduction.

There is a number of theoretical methods [14–16] that take account of N-processes. The Callaway method is most suitable for our purpose. The experimental results are described using the Callaway relaxation method [16] within the Debye model. The Callaway expression for the thermal conductivity of a dielectric crystal can be written as

$$\kappa = \kappa_1 + \kappa_2, \quad (1)$$

where

$$\kappa_1 = GT^3 \int_0^{\Theta/T} \tau_c f(x) dx, \quad (2)$$

$$\kappa_2 = GT^3 \left(\int_0^{\Theta/T} \frac{\tau_c}{\tau_N} f(x) dx \right)^2 \left(\int_0^{\Theta/T} \frac{\tau_c}{\tau_N \tau_R} f(x) dx \right)^{-1}. \quad (3)$$

Here

$$G = \frac{k_B^4}{2\pi^2 v \hbar^3}, \quad f(x) = \frac{x^4 e^x}{(e^x - 1)^2},$$

$x = \hbar\omega/k_B T$ is the dimensionless variable, k_B is the Boltzmann constant, \hbar is the Planck constant, ω is the phonon frequency. Θ is the characteristic Debye temperature, τ_R , τ_N are the relaxation times for «resistive» and normal interaction processes, τ_c is the combined phonon relaxation time, $v = [(v_l^{-3} + 2v_t^{-3})/3]^{-1/3}$ is the sound velocity averaged over the longitudinal v_l and transverse v_t polarizations [17].

The low-temperature results were analyzed disregarding either librations or phonon scattering on librations because the lowest-energy excitation level of librations is about 105 K (CO₂) and 100 K (N₂O) [2].

Assuming that different types of scattering are independent, the relaxation times τ_c and τ_R can be written as

$$\tau_c^{-1} = \tau_R^{-1} + \tau_N^{-1}, \quad (4)$$

$$\tau_R^{-1} = \sum \tau_i^{-1}. \quad (5)$$

Here τ_i^{-1} ($i = b, p, d, u$) denotes the relaxation times for different phonon-scattering mechanisms. The temperature and frequency dependence of the relaxation times [14] for phonon scattering at grain boundaries, stress fields of dislocations, isotopic impurities and in the U-processes are as follows:

$$\begin{aligned} \tau_b^{-1} &= a_b; \quad \tau_d^{-1} = a_d x T; \quad \tau_p^{-1} = a_p x^4 T^4; \\ \tau_u^{-1} &= a_{1u} x^2 T^5 \exp(-a_{2u}/T). \end{aligned} \quad (6)$$

The role of normal processes for low-energy phonons was investigated by Herring [18]. He found that the relaxation time of normal processes involving acoustic phonons in the high-symmetry (cubic) crystals at low temperatures can be written as

$$\tau_N^{-1} \propto \omega^2 T^3 \propto x^2 T^5. \quad (7)$$

Later, rather elaborate expressions (e.g., see Ref. 19) were obtained for relaxation times, which took into account the phonon polarization in different processes of phonon decay/production ($l \leftrightarrow l+t$, $l \leftrightarrow t+t$, etc.) as a function of temperature and frequency. The thermal conductivity asymptotes obtained (both for low and high temperatures) have extremely limited areas of applicability, well beyond the temperature range of experiment. Usually, the polarization-averaged relaxation rate for N-processes is obtained from the analysis of thermal conductivity experimental results for cryocrystals. The inverse relaxation time $\tau_N^{-1}(\omega, T)$ is therefore found using expressions with fitting parameters [11,14,18–21]. However, comparison with low-temperature experiment is most often made using Eq. (7) and neglecting the contribution of transverse phonons (e.g., see Refs. 18, 21). To analyze our experimental results, we used Eq. (7) and other expressions [11,19,20] as trial functions.

Our results were approximated using the procedure from [11]. The parameters a_j ($j = b, p, d, 1u, 2u, N$) were estimated through minimizing the functional $\sum_i [(\kappa_{ci} - \kappa_{ei})/\kappa_{ei}]^2$, where κ_{ci} and κ_{ei} are the calculated and experimental thermal conductivity coefficients, respectively, at the i -th point.

The calculation was performed using the following values [2]: $\Theta = 141$ K, $v_l = 2676.3$ m/s, $v_t = 1513.1$ m/s for N₂O, and $\Theta = 151.8$ K, $v_l = 2806.4$ m/s, $v_t = 1605.7$ m/s for CO₂.

The fitting to the experimental temperature dependence of the thermal conductivity of crystalline CO₂ was best described by Eq. (1) with

$$\begin{aligned} \tau_R^{-1} &= 1.07 \cdot 10^5 + 1.9 x^4 T^4 + 8.4 \cdot 10^4 x T + \\ &+ 781 x^2 T^5 \exp(-23.8/T); \\ \tau_N^{-1} &= 1.62 \cdot 10^3 x^2 T^5. \end{aligned} \quad (8)$$

The relaxation times providing the best description of the fitting for N₂O are

$$\tau_R^{-1} = \tau_b^{-1} + \tau_p^{-1} + \tau_d^{-1} + \tau_u^{-1} + \tau_a^{-1}, \quad (9)$$

and τ_N^{-1} is given by Eq. (7).

The term τ_a^{-1} is introduced into Eq. (9) to take into account the extra (compared to CO₂) phonon scattering. We assume that the extra scattering is caused by the low-frequency excitations related to the orientational subsystem

of N₂O. The relaxation rate τ_a^{-1} of the acoustic phonons can be written within the SPM [9] model as

$$\tau_a^{-1} = c_1 x T \tanh \frac{x}{2} + c_2 (xT)^4 + c_3 x T^3. \quad (10)$$

The first term describes the resonance phonon scattering on the tunnel states of two-level systems. The other terms concern scattering on low-energy soft quasiharmonic oscillations.

Applying the approximation procedure, we could estimate the scattering intensities:

$$\begin{aligned} \tau_R^{-1} = & 4.47 \cdot 10^5 + 5.77(xT)^4 + 1.06 \cdot 10^3 x T + \\ & + 1.63 \cdot 10^3 x^2 T^5 \exp(-10.39/T) + 2.7 \cdot 10^5 x T \tanh \frac{x}{2} + \\ & + 43(xT)^4 + 3.22 \cdot 10^4 x T^3, \end{aligned} \quad (11)$$

$$\tau_N^{-1} = 2.7 \cdot 10^3 x^2 T^5. \quad (12)$$

Figure 1 shows the approximation curves (solid lines) that provide the best description of the experimental results on the thermal conductivity of N₂O and CO₂. It is seen that below 20 K the description is quite good.

The coefficients in the summands (which describe phonon scattering on grain boundaries, stress fields of dislocations, and in U-processes) of Eqs. (8) and (11) testify that in both CO₂ and N₂O solids indicate large size of crystalline grains, low density of dislocations, and weak phonon–phonon interaction. These might be reasons for the good thermal conduction in these crystals at temperatures near the maximum.

We assume that the differences in the low-temperature thermal conductivity of these crystals are due to this phonon scattering τ_a^{-1} , Eq. (10). If we add this contribution τ_a^{-1} of Eq. (10) to the fitting procedure CO₂, the resulting curve will describe well the temperature dependence of the thermal conductivity of N₂O. Indeed, Fig. 2 illustrates the experimental temperature dependences of the thermal conductivity of the CO₂ and N₂O crystals. It also shows hypothetical curves 1 (dashed line) and 2 (solid line). Curve 1 was obtained as follows. The thermal conductivity κ was calculated from Eq. (1) for CO₂ using the relaxation times given in Eq. (8). In this procedure the term τ_a^{-1} of Eq. (10) with the coefficients c_i obtained in Eq. (11) by approximating the curve for N₂O was introduced into the term τ_R^{-1} of Eq. (8) for CO₂. It is seen that hypothetical curve 1 provides a qualitatively adequate description of the thermal conductivity of N₂O below the maximum. Curve 1 can be transformed into curve 2 by taking into account the difference of the parameters of the U-processes in N₂O. Hypothetical curve 2 describes qualitatively the temperature dependence of N₂O. The expression τ_a^{-1} , Eq. (10), thus permits us to describe effectively the extra (as compared to CO₂) phonon scattering in the

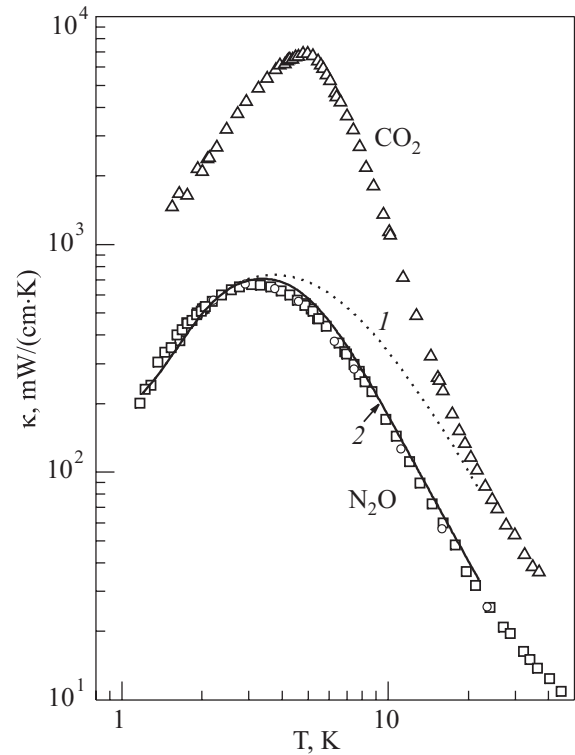


Fig. 2. Thermal conductivity of CO₂ and N₂O solids. Experiment: N₂O (□, ○), CO₂ (△). Calculation: curves 1 and 2. The explanation is in the text.

N₂O crystal. It is a very surprising result. The phonon scattering on low-energy excitations, associated with the frozen disordered orientations of N₂O molecules, have a glass-like character in the crystalline N₂O.

The intensity of N-processes can be expressed in terms of the characteristics of the crystal [21]. To estimate the intensity of normal phonon scattering, we used for τ_N^{-1} the expression [19–21]

$$\tau_N^{-1} \approx b \left(\frac{\omega}{\omega_D} \right)^2 \left(\frac{T}{\Theta} \right)^3, \quad b \cong \frac{16\pi^3}{735\sqrt{3}} \frac{\gamma^2 R_0^3 \hbar}{M} \left(\frac{k\Theta}{\hbar v_t} \right)^5, \quad (13)$$

where R_0 is the distance between nearest neighbors, M is the molecular mass, γ is the Grüneisen constant. Equation (13) can be rewritten as

$$\tau_N^{-1} = A_N x^2 T^5 \quad (14)$$

with

$$A_N = 1.27 \cdot 10^9 \frac{\gamma^2}{\mu V^{2/3} \Theta^5}, \quad (15)$$

where μ and V are the molar mass and volume, respectively. According to Eq. (15), the intensity of normal processes A_N is determined by the physical parameters of the substance. The intensities of obtained from experiment

and calculated from Eq. (15) are given in Table 1. We see quite a good agreement.

Table 1. The intensities of normal processes, resulting from thermal conductivity experiment and calculations according to Eq. (15).

	μ , 10^{-3} kg/mole	Γ	V , 10^{-6} m ³ /mole	Θ , K	A_N , 10^3 s ⁻¹ K ⁻⁵	
					experiment	calculation
CO ₂	44	2.13	25.796	151.8	1.62	1.86
N ₂ O	44	2.16	27.018	141.0	2.70	2.69

The dependence on the Debye temperature in the coefficient A_N can be separated:

$$A_N^* = A_N \gamma^{-2} \mu V^{2/3} \propto \Theta^{-5}. \quad (16)$$

Figure 3 illustrates the normal process intensities in logarithmic coordinates ($A_N^* = A_N \gamma^{-2} \mu V^{2/3}$ in reduced coordinates) for CO₂ and N₂O as a function of the Debye temperature. It also shows literature data for the hydrogens [21,22] and Ne [23]. It is seen that the reduced intensity of normal processes A_N^* is inversely proportional to Θ^5 for CO₂, N₂O and Ne crystals. This power law holds for the hydrogens [21,22] to within a constant factor ($2\sqrt{2}$).

So, comparison between calculated and experimental values of the intensity of normal phonon scattering in CO₂ and N₂O shows that they are determined by the physical parameters of the substance.

Conclusions

Thermal conductivities of the CO₂ and N₂O crystals have been measured in the temperature interval 1–40 K. A technique has been developed that permitted us to grow perfect samples of solid CO₂ and N₂O. It is found that both CO₂ and N₂O have very high thermal conductivities at the maxima but differ surprisingly widely from each other. The experimental temperature dependence of the thermal conductivity is described using the Callaway relaxation method within the Debye model. Analysis of the experimental results shows that relatively large size of crystalline grains, low density of dislocations and weak

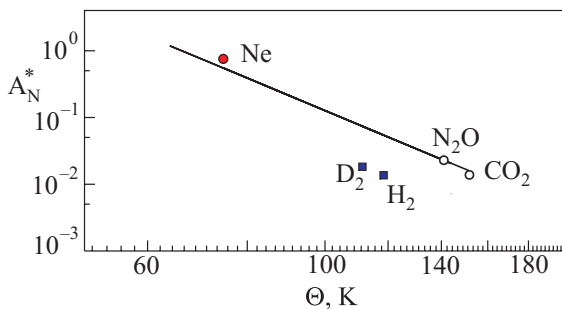


Fig. 3. Dependence of reduced intensity of normal processes for molecular cryocrystals CO₂ and N₂O on Debye temperature. The data for Ne, H₂, D₂ are taken from the of Refs. 21–23.

phonon–phonon interaction might be reasons for the good thermal conduction in these crystals at temperatures near the thermal conductivity maximum. It is shown that the normal process intensities in these cryocrystals are determined by the physical parameters of the substances. In N₂O solid there is a very large extra (as compared to CO₂) contribution to the phonon scattering at temperatures near the thermal conductivity maximum. This scattering is described within the model of soft potentials by the resonance phonon scattering at the tunnel states and low-energy quasiharmonic oscillations.

The authors gratefully thank Yu.A. Freiman, B.Ya. Gorodilov and M.A. Strzhemechny for fruitful discussion.

1. *Cryocrystals*, B.I. Verkin and A.F. Prichot'ko (eds.), Naukova Dumka, Kiev (1983) [in Russian].
2. *Physics of Cryocrystals*, V.G. Manzhelii and Yu.A. Freiman (eds.), AIP, New York (1996).
3. K.R. Nary, P.L. Kuhns, and M.S. Conradi, *Phys. Rev.* **B26**, 3370 (1982).
4. T. Atake and H.A. Chihara, *Bull. Chem. Soc. Jpn.* **47**, 2126 (1974).
5. V.V. Sumarokov, P. Stachowiak, and A. Jeżowski, *Fiz. Nizk. Temp.* **29**, 603 (2003) [*Low Temp. Phys.* **29**, 449 (2003)].
6. P. Stachowiak, V.V. Sumarokov, J. Mucha, and A. Jeżowski, *Phys. Rev.* **B67**, 172102 (2003).
7. V.V. Sumarokov, P. Stachowiak, J. Mucha, and A. Jeżowski, *Phys. Rev.* **B74**, 224302 (2006).
8. P.W. Anderson, B.I. Halperin, and C.M. Varma, *Philos. Mag.* **2**, 1 (1972); W.A. Phillips, *J. Low Temp. Phys.* **7**, 351 (1972).
9. D.A. Parshin, *Fiz. Tv. Tela* **36**, 1809 (1994).
10. A. Jeżowski and P. Stachowiak, *Cryogenics* **32**, 601 (1992).
11. P. Stachowiak, V.V. Sumarokov, J. Mucha, and A. Jeżowski, *Phys. Rev.* **B50**, 543 (1994).
12. P. Stachowiak, V.V. Sumarokov, J. Mucha, and A. Jeżowski, *J. Low Temp. Phys.* **111**, 379 (1998).
13. A. Jeżowski, P. Stachowiak, V.V. Sumarokov, J. Mucha, and Yu.A. Freiman, *Phys. Rev. Lett.* **71**, 97 (1993).
14. R. Berman, *Thermal Conduction in Solids*, Clarendon, Oxford (1976).
15. R.A. Guyer and I.A. Krumhansl, *Phys. Rev.* **148**, 766 (1966); *ibid.* **148**, 778 (1966).
16. J. Callaway, *Phys. Rev.* **113**, 1046 (1959).
17. T.A. Scott, *Phys. Rep.* **C27**, 89 (1976).
18. C. Herring, *Phys. Rev.* **95**, 54 (1954).
19. T.N. Antsygina and V.A. Slusarev, *Fiz. Nizk. Temp.* **19**, 494 (1993) [*Low Temp. Phys.* **19**, 348 (1993)].
20. T.N. Antsygina, B.Ya. Gorodilov, N.N. Zholonko, A.I. Krivchikov, V.G. Manzhelii, and V.A. Slusarev, *Fiz. Nizk. Temp.* **18**, 417 (1992) [*Low Temp. Phys.* **18**, 283 (1992)].
21. O.A. Korolyuk, B.Ya. Gorodilov, A.I. Krivchikov, and V.V. Dudkin, *Fiz. Nizk. Temp.* **26**, 323 (2000) [*Low Temp. Phys.* **26**, 235 (2000)].
22. B.Ya. Gorodilov, A.I. Krivchikov, V.G. Manzhelii, and N.N. Zholonko, *Fiz. Nizk. Temp.* **20**, 78 (1994) [*Low Temp. Phys.* **20**, 66 (1994)].
23. R.M. Kimber and S.J. Rogers, *J. Phys. C: Solid State Phys.* **6**, 2279 (1973).